

1 **Probing the limit of hydrologic predictability with the Transformer network**

2

3 Jiangtao Liu¹, Yuchen Bian², Kathryn Lawson¹, and Chaopeng Shen^{*,1}

4 ¹Civil and Environmental Engineering, The Pennsylvania State University

5 ²Amazon Search Science and AI

6 * Corresponding author: Chaopeng Shen, cshen@engr.psu.edu

7

8 **Keywords:** Transformer, long short-term memory, streamflow, CAMELS, deep learning

9

10

11

12

13 **Abstract**

14 For a number of years since their introduction to hydrology, recurrent neural networks like long
15 short-term memory (LSTM) networks have proven remarkably difficult to surpass in terms of daily
16 hydrograph metrics on community-shared benchmarks. Outside of hydrology, Transformers have
17 now become the model of choice for sequential prediction tasks, making it a curious architecture
18 to investigate for application to hydrology. Here, we first show that a vanilla (basic) Transformer
19 architecture is not competitive against LSTM on the widely benchmarked CAMELS streamflow
20 dataset, and lagged especially prominently for the high-flow metrics, perhaps due to the lack of
21 memory mechanisms. However, a recurrence-free variant of the Transformer model can obtain
22 mixed comparisons with LSTM, producing very slightly higher Kling-Gupta efficiency coefficients
23 (KGE), along with other metrics. The lack of advantages for the vanilla Transformer network is
24 linked to the nature of hydrologic processes. Additionally, similar to LSTM, the Transformer can
25 also merge multiple meteorological forcing datasets to improve model performance. Therefore,
26 the modified Transformer represents a rare competitive architecture to LSTM in rigorous
27 benchmarks. Valuable lessons were learned: (1) the basic Transformer architecture is not suitable
28 for hydrologic modeling; (2) the recurrence-free modification is beneficial so future work should
29 continue to test such modifications; and (3) the performance of state-of-the-art models may be
30 close to the prediction limits of the dataset. As a non-recurrent model, the Transformer may bear
31 scale advantages for learning from bigger datasets and storing knowledge. This work lays the
32 groundwork for future explorations into pretraining models, serving as a foundational benchmark
33 that underscores the potential benefits in hydrology.

34

35

36 ***Introduction***

37 Rainfall-runoff modeling is essential for flood prediction, water resource management, and
38 environmental protection (Hrachowitz & Clark, 2017). Rainfall-runoff modeling is a critical aspect
39 of hydrology, as it models the intricate relationships between precipitation, watershed
40 characteristics, and streamflow. The introduction of long short-term memory (LSTM) networks
41 marked a significant advancement in this field for numerous variables of interest including soil
42 moisture (Fang et al., 2017; J. Liu et al., 2022, 2023), streamflow (Botterill & McMillan, 2023; Feng
43 et al., 2020, 2021; Konapala et al., 2020; Kratzert et al., 2019; Sun et al., 2021; Xiang & Demir,
44 2020), water temperature (Rahmani, Lawson, et al., 2021; Rahmani, Shen, et al., 2021), and
45 groundwater levels (Afzaal et al., 2020; Wunsch et al., 2022). For these applications, LSTM
46 consistently outperformed traditional models and process-based models (Feng et al., 2020;
47 Papacharalampous et al., 2018). LSTM's ability to learn many-step dependencies and handle
48 variable-length input sequences has proven particularly advantageous in capturing the inherent
49 complexity of hydrological processes (Hochreiter & Schmidhuber, 1997).

50

51 As a recurrent neural network (RNN), LSTM processes data sequentially through time steps,
52 updating its internal states at each step based on the current input and the previous states. This
53 iterative process, which involves repeatedly applying its internal neural network mechanisms,
54 leads to some limitations. The recurrent nature means RNNs are prone to an issue called the
55 vanishing gradient (Hochreiter, 1991; Hochreiter et al., 2001), where the gradient of the loss with
56 respect to the network weights becomes very small, making network training extremely slow. This
57 issue limits the length of the training sequence, and reduces the impact of inputs from the longer-
58 term past on present predictions. This could be one of the reasons why baseflow was previously
59 identified as a limitation (Feng et al., 2020). Even though LSTM was developed to mitigate this
60 issue and can suppress it better than the original RNNs, it is not immune to it (Dai et al., 2019;

61 Zhang et al., 2016). Furthermore, recurrence means these time steps must be taken in sequence
62 --- the time steps cannot be run in parallel. This imposes a restriction on the efficiency of parallel
63 processing, and thus the scale of data on which the model can be trained.

64

65 In many applications outside hydrology, the Transformer architecture (Vaswani et al., 2017) has
66 demonstrated superior performance over LSTM networks in various domains, including machine
67 translation, speech recognition (Karita et al., 2019), natural language processing and sentiment
68 analysis (Devlin et al., 2019), question answering (Rajpurkar et al., 2018), computer vision (Carion
69 et al., 2020), protein structure prediction (Rives et al., 2021), and music generation (Huang et al.,
70 2018). The Transformer model uses an attention mechanism, where each word (or "input token")
71 is transformed into three different kinds of information: a 'query' that asks how relevant other
72 words are to it, a 'key' that responds to others' queries about its relevance, and a 'value' that
73 carries the word's actual meaning. The model calculates the relevancies between the query and
74 keys of all words, then combines the values of the most relevant words to understand the current
75 word better. With LSTM, the most recent input tokens are always more important than further-
76 away ones, whereas a Transformer could learn to put more focus on further-away tokens
77 (Dehghani et al., 2019; Raganato & Tiedemann, 2018), which makes it ideal for language
78 modeling. Moreover, as it does not have recurrence, a Transformer can run the time steps in
79 parallel and can scale up in parallel computation when more data and more GPUs are available.
80 Considering such benefits, there should be a heightened interest in harnessing Transformers for
81 hydrologic applications. Transformers are increasingly being used in hydrologic and water quality
82 modeling (Castangia et al., 2023; Koya & Roy, 2023; Li & Yang, 2019; Xu et al., 2021; H. Yang
83 et al., 2023), especially for near-term forecasting. However, the scale of application tends to be
84 limited and their benchmarking on standardized, well-understood datasets, such as the
85 Catchment Attributes and Meteorology for Large-sample Studies (CAMELS) dataset (Addor et al.,
86 2017; Newman et al., 2014), remains limited in the literature. It is thus intriguing whether the

87 Transformer's advantages over recurrent networks will apply in the case of natural systems, which
88 can be argued to lack the irregular sequential structure found in human languages.

89

90 While some past hydrologic studies have claimed superior performance for some other
91 architectures compared to LSTM, many times, a rigorous comparison was not carried out due to
92 the different modeling objectives. The conclusions were often conditional on using a small dataset
93 for benchmarking, e.g., see (Abed et al., 2022; Amanambu et al., 2022; Ghobadi & Kang, 2022),
94 using procedures and configurations (training and test periods, sites, and forcing data) that are
95 different from published benchmarks (Yin et al., 2022, 2023), or on a case study which was not
96 easy to compare to the work of other independent teams (Koya & Roy, 2023; C. Liu et al., 2022).

97 Specifically, Yin et al. (2022) proposed the RR-Former model (a transformer variant) and
98 conducted experiments with 7-day forecasts on the CAMELS dataset. They modeled 673 distinct
99 basins independently and calculated performance metrics for each, and they also assessed a
100 selected set of 448 basins using a single model. In contrast, our research primarily focuses on
101 long-term prediction problems rather than forecasting. Forecasting typically involves predicting
102 results within a relatively short period based on historical data, whereas our study concentrates
103 on the long-term rainfall-runoff relationship to better understand its underlying patterns. Building
104 on the work by Yin et al. (2022), Yin et al. (2023) introduced the RRS-Former model, which
105 conducted a one-day-ahead runoff experiment. A similar study by (Feng et al., 2020) applied a
106 data integration approach to an LSTM model. Although direct comparison is challenging, Feng et
107 al. (2020) reported a median NSE of 0.86, which was superior to the RRS-Former model's
108 performance in Yin et al. (2023). Koya and Roy (2023) evaluated the Temporal Fusion
109 Transformer (TFT) model on the Caravan dataset (Kratzert et al., 2023) and reported median
110 Kling Gupta efficiency (KGE) of 0.705. However, Feng et al., (2023) benchmarked LSTM on a
111 similarly large dataset and showed median KGEs of 0.74 for 3753 global basins and 0.78 for 1675
112 basins with long-term records. Furthermore, while more benchmarking is welcomed, the model in

113 Koya and Roy (2023) is not purely attention-based, as it incorporates some LSTM layers in its
114 encoder, making it difficult to determine whether the performance improvements are due to the
115 attention mechanism or the LSTM layers. This approach also brought back time recurrence and
116 did not leverage the time parallelism of the transformer network as advocated in the original
117 transformer model. In the interest of reproducibility and comparability, which underpin scientific
118 progress, it is useful to benchmark under similar conditions, on the same (reasonably large)
119 dataset. Data-driven deep learning models enjoy the feature of “data synergy”, where larger and
120 more diverse data leads to stronger and more robust models (Fang et al., 2022; Kratzert et al.,
121 2021; Pasquiou et al., 2022; E. Yang et al., 2023). Thus small-data comparison results may not
122 be valid for a case with more data. Thus far, on the CAMELS dataset (Addor et al., 2017; Newman
123 et al., 2014), both Kratzert et al. (2019) and Feng et al. (2021) reported very similar metric Nash-
124 Sutcliffe model efficiency coefficient (NSE) (Nash & Sutcliffe, 1970) for LSTM --- 0.72 for 571
125 basins with the NLDAS forcing alone, making this a reliable benchmark that has thus far not been
126 exceeded by other models. Sun et al. (2021) reported comparable results using GraphWaveNet,
127 although with different training periods and ensemble setups. Furthermore, Kratzert
128 simultaneously employed multiple forcing dataset (NLDAS, Maurer, and Daymet) for LSTM and
129 obtained a Kling-Gupta model efficiency coefficient (KGE) (Gupta et al., 2009) of 0.80, which is
130 the record on this dataset that no other model has matched.

131
132 In this study, we investigate the performance of the Transformer architecture in rainfall-runoff
133 modeling compared to LSTM using the CAMELS dataset. We analyze the performance of single
134 models and ensembles for both architectures, and examine the models' ability to handle multiple
135 forcings and mixed forcing cases. This approach aims to establish a reference point for future
136 studies to compare, enhancing our understanding of these models in complex scenarios. Our
137 findings contribute to the understanding of the strengths and limitations of both LSTM and

138 Transformer models in hydrological predictions, and highlight the potential of the Transformer as
139 an alternative and scalable solution for hydrologic modeling.

140

141 ***Data and Methods***

142

143 **Datasets**

144 In this paper, we utilized the Catchment Attributes and Meteorology for Large-sample Studies
145 (CAMELS) dataset (Addor et al., 2017; Newman et al., 2014), which includes basin-averaged
146 daily data from 671 catchments across the conterminous United States (CONUS) characterized
147 by minimal anthropogenic disturbances. The catchment attributes encompass an array of
148 characteristics such as topography, soil properties, and geological aspects. Furthermore,
149 CAMELS provides daily meteorological forcing inputs derived from three distinct gridded data
150 products, namely Daymet (Thornton et al., 1997), Maurer (Maurer et al., 2002), and the North
151 American Land Data Assimilation System (NLDAS) (Xia et al., 2012).

152

153 **Vanilla (basic) Transformer models**

154 The Transformer model, as first introduced in the paper “Attention is all you need” by Vaswani et
155 al. (2017), is a neural network architecture for sequential data processing. The Transformer model
156 consists of an encoder and a decoder. The encoder has a number (n_{layer}) of stacked encoding
157 layers (“stacked” means the output of one layer becomes the input to the next one), each of which
158 consists of a self-attention layer and a position-wise fully connected layer, while the decoder has
159 only a simple position-wise linear layer. The critical mechanism within the encoder is self-attention,
160 which computes the weighted sum of all input features. The equations for one of the stacked
161 encoding layers are shown below and explain the calculations one by one.

162

$$Q = x * D(W_q) \quad (1)$$

$$K = x * D(W_k) \quad (2)$$

$$V = x * D(W_v) \quad (3)$$

$$a = \text{softmax} \left(\frac{QK^T}{\sqrt{d_k}} \right) \quad (4)$$

$$c = a * V \quad (5)$$

$$u' = c * W_o \quad (6)$$

$$u = \text{BatchNorm}(x + D(u')) \quad (7)$$

$$z' = W_2 * D(\text{GELU}(W_1 * u)) \quad (8)$$

$$z = \text{BatchNorm}(u + z') \quad (9)$$

163 The inputs x to the attention layer have two dimensions --- the sequence length (n) and a hidden-
 164 size dimension (d_k). In Equations (1-3), the layer computes three sets of linear transformations,
 165 called Query, Key, and Value vectors (Q, K, V), and W_q, W_k , and W_v , all with the dimensions (d_k ,
 166 d_k), represent the respective learnable weights. These position-wise transformations (or matrix
 167 multiplications) mix information along the hidden-size dimension, not along the sequence length
 168 dimension, while applying the dropout operator $D()$. To mitigate overfitting, a dropout mask with
 169 a ratio of 0.5 is applied to W_q, W_k , and W_v . Equation 4 computes the dot product of Query and
 170 Key, and obtains a matrix of the size (n, n) which tabulates the similarity between each Query-
 171 Key pair. It then scales the calculations by $\sqrt{d_k}$, before applying the softmax operation along the
 172 sequence dimension. The output a is the above-mentioned attention weight while c is the
 173 attention-weighted values, called “contexts”. The model is called “multiheaded” in that multiple
 174 sets of Q, K, V are computed and their results c are concatenated as c before applying a linear
 175 layer in Equation 6. Equations 7-9 apply additional linear layers with activation functions and
 176 residual connections to enhance training. z' is a feed-forward neural network (FFN) consisting of
 177 two linear transformations with a Gaussian Error Linear Unit (GELU) activation function in
 178 between. z includes a residual connection and batch normalization, where the elements along the

179 batch dimension is normalized. As described earlier, Equations 1-9 are repeated n_{layer} times and
180 the outputs of one layer serves as the inputs to the subsequent layer. The dimensional
181 descriptions here all ignore the batch dimension (a collection of instances to compute a loss value
182 and update the weights) which is in practice computed in parallel. The sequence length (n), the
183 number of heads (h) and the hidden size (d_k) are hyperparameters to be tuned using the validation
184 dataset.

185

186 Equations (4-5) can be interpreted as weighing every token in the sequence to make a combined
187 prediction at a given location. We observe that, unlike RNNs which would naturally put more
188 weight to adjacent tokens, the sense of adjacency is lost for the attention layer --- for prediction
189 location i , all input tokens are treated equally, regardless whether they are close or far from i . The
190 larger focus to adjacent tokens, if it exists in the training dataset, is completely obtained from data.
191 Furthermore, any relational structure in the sequence dimension is not modeled --- the softmax
192 operator in Equation 4 is the only operator that mixes information over the sequence length, as
193 all the other operators are calculated in parallel for each token in the sequence. This setup is
194 reasonable in language modeling where inversion structures are common, but may not be optimal
195 if the proximity is important as in natural physical processes. However, stacking many layers of
196 attention sequentially as done in the Transformer could enable the modeling of some sequential
197 structure.

198

199 The initial input to the model, X , is of dimension (n, n_x) , which is transformed by an embedding
200 function. It includes three parts: a linear layer transformation of the inputs, a “positional embedding”
201 (Equation 10-11), and a “temporal embedding” (Equation 12-13). These three components are
202 directly summed to obtain the input x in Equations 1-3 which is then fed into the attention layers
203 described above. The embeddings are added because the Transformer does not inherently
204 account for the positional information. The positional encoding uses sine and cosine functions to

205 create a unique encoding for each position, allowing the model's self-attention mechanism to
206 maintain the sequence order in context (Vaswani et al., 2017):

207

$$P_{k,2i} = \sin\left(\frac{k}{10000^{2i/d}}\right) \quad (10)$$

$$P_{k,2i+1} = \cos\left(\frac{k}{10000^{2i/d}}\right) \quad (11)$$

208 where k is the position in the sequence, i is the dimension, and d is the number of columns in the
209 embedding matrix.

210

211 Furthermore, in the time series data, positional embedding alone can hardly reflect the seasonality
212 information. Hence, hierarchical global timestamp information (weekly, monthly, yearly) is used
213 to encode seasonality and long-term ordinal information (Zhou et al., 2021). This temporal
214 embedding calculates and normalizes the day of the week, day of the month, and day of the year
215 for each time period to a range of -0.5 to 0.5:

216

$$d_i(k) = t_i(k)/N_i - 0.5 \quad (12)$$

$$T_e(k) = \bigoplus_{\{i \in \text{time_features}\}} d_i(k) \quad (13)$$

217

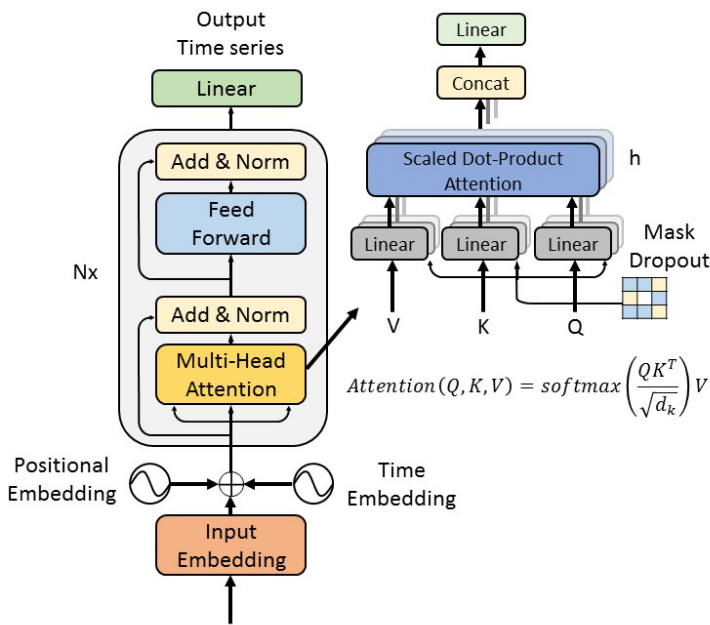
218 where t_i is the value of time feature i at position k in the sequence; for example, day of the week,
219 day of the month, or day of the year. N_i is the total number of values for the time feature i ; for
220 example, for the day of the year i , N_i would be 365. d_i is the normalized value for each time
221 feature. $T_e(k)$ indicates the temporal embedding at position k . The ' \oplus ' symbol denotes
222 concatenation, meaning it concatenates the time features into a single vector at the last dimension.

223

224 Positional and temporal embeddings are added to the input embeddings to form the input to the
 225 transformer layer.

$$x = E_X(X) + E_P(P) + E_T(T) \quad (14)$$

226 where E_X , E_P , E_T are the learned linear embedding layers projecting the inputs to the model
 227 hidden dimension, respectively.



228
 229 *Figure 1. The base Transformer model structure (adapted from Figure 1 in Vaswani et al., 2017)*
 230 *used in this paper.*

231

232

233 The Modified Transformer Model with Convolutional Embeddings

234 As a variant of the Transformer model, we added a one-dimensional convolutional embedding
 235 layer just before the attention layer to produce relational features in the time dimension. In this
 236 embedding layer, two stacked convolution sub-layers were introduced, with residual
 237 connections between them, and their outputs are fed into a linear layer. In each convolutional
 238 sub-layer, the time sequence length dimension gets convolved and, as such convolutions are
 239 non-recurrent, the model does not need to go through time steps in order to represent the

240 temporal relational structures. The convolutional sub-layers have a dilation of 1, a stride of 1,
241 ReLU as the activation functions, and a backward-focusing kernel to ensure that inputs from the
242 future do not get used to make a prediction of the current time step. The kernel width, hidden
243 sizes and the number of convolutional layers were set as hyperparameters that were tuned
244 along with the hyperparameters of the attention layers. The outputs of the whole convolutional
245 embedding layer are, along with the time positional and temporal embeddings, added to the
246 input embeddings just as in Equation (14).

247

248 **LSTM Models and SAC-SMA Models**

249

250 In order to impartially evaluate the Transformer model's performance, we compared its results
251 with those of LSTM and the Sacramento Soil Moisture Accounting (SAC-SMA) conceptual model
252 (Anderson & McDonnell, 2005; Burnash et al., 1973), and used the latter two as benchmarks. We
253 downloaded the SCA-SMA dataset from HydroShare (Kratzert et al., 2019), and set the same test
254 time for all models to ensure a balanced comparison. This approach helps provide a thorough
255 and fair assessment of each model's performance capabilities. The LSTM model's configurations
256 were based on Kratzert et al. (2021), with the models' hyperparameters set to 30 epochs, a
257 sequence length of 365, a hidden size of 256, and a dropout rate of 0.4.

258

259 The LSTM model from Kratzert et al., 2019 was originally evaluated on 531 basins. To broaden
260 our insights into the impacts of a single forcing dataset on the entire CAMELS dataset and ensure
261 a fair comparison, we retrained their model on the full set of 671 basins with the single NLDAS
262 forcing dataset. We further attempted to incorporate time stamp information as inputs into the
263 LSTM model (data not shown). However, this did not lead to any improved performance,
264 suggesting it does not introduce new information to LSTM.

265

266 **Experiments and Model Evaluation**

267

268 To enable a comprehensive comparison with various benchmarks, we utilized data from all 671
269 CAMELS basins. To be consistent with previous benchmark experiments, we employ both single
270 and multi-forcing datasets, in the same manner as the benchmark (Kratzert et al., 2021). Initially,
271 we applied a single forcing dataset derived from NLDAS, referred to as the 'single-forcing'
272 experiment. Subsequently, we conducted a multi-forcing analysis using forcing data from Daymet,
273 Maurer, and NLDAS. For this analysis, our scope was narrowed to 531 basins. It should be noted
274 that the variable selection and settings for the model input data were chosen to be consistently
275 aligned with those employed by Kratzert et al. (2021).

276

277 For all models, the data used for the training period was from 1 October 1999 to 30 September
278 2008, while the data used for the testing period was from 1 October 1989 to 30 September 1999.
279 During the training period, the weights were optimized using the Adam optimizer with a learning
280 rate of 0.0001.

281

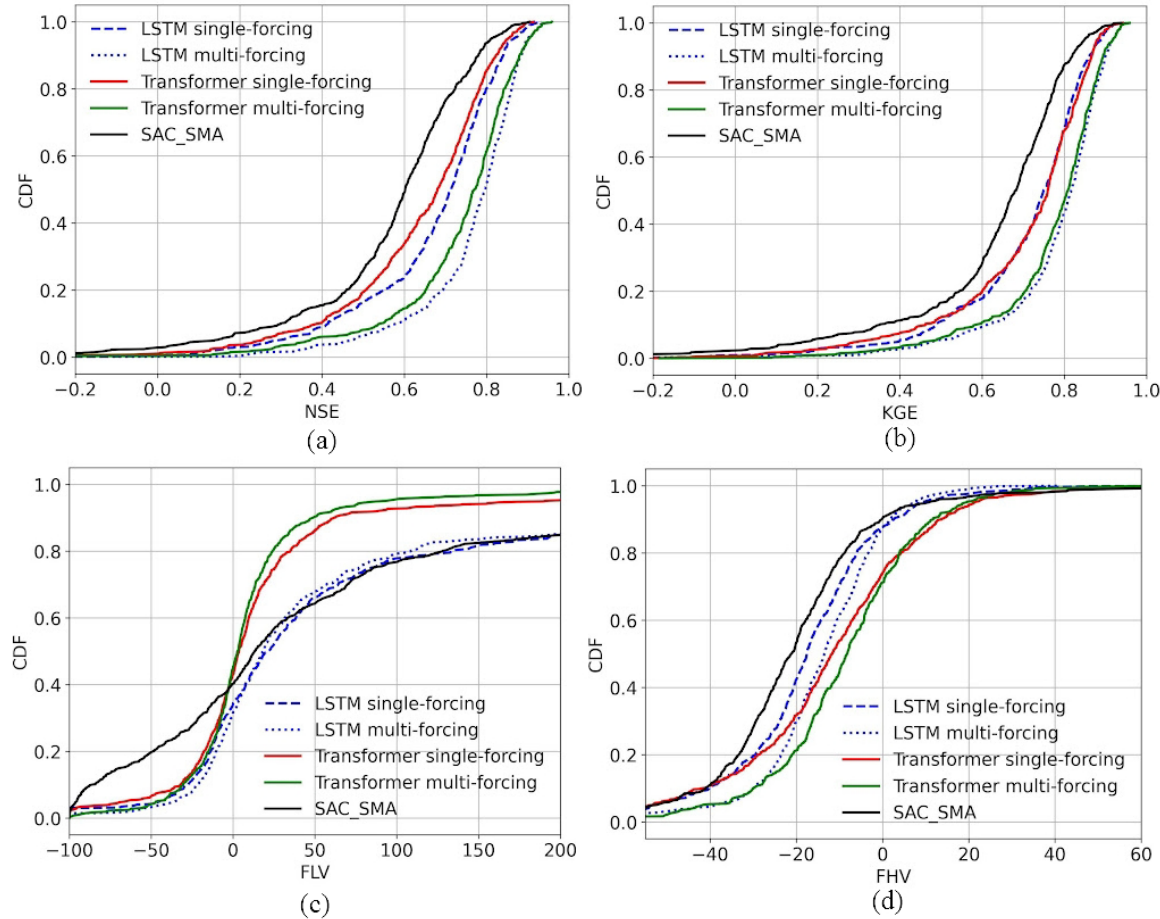
282 To accurately compare different model architectures and hyperparameters, we used one specific
283 seed in Figure 2. Thus any differences in model performance can be fully attributed to the specific
284 architectural or hyperparameter variations. To increase the robustness of the analysis, we
285 employed an ensemble approach, using ten simulations with different random seeds for each of
286 the model architectures. The ensemble-averaged discharge for each model architecture is what
287 is presented in the results here, as it not only helps to capture the variation in results due to
288 randomness, but also provides more stable performance estimates.

289

290 We evaluated model performance using several metrics, including the Nash-Sutcliffe model
291 efficiency coefficient (NSE) (Nash & Sutcliffe, 1970) and the Kling-Gupta model efficiency

292 coefficient (KGE) (Gupta et al., 2009). We also considered the percent bias of the top 2% peak
 293 flow range (FHV) and the bottom 30% low flow range (FLV), which respectively highlight model
 294 performance for peak flows and baseflow (Yilmaz et al., 2008).

295
 296
 297 **Results and Discussion**
 298



299
 300 *Figure 2. Comparative analysis of Cumulative Density Function (CDF) across various models*
 301 *including Long Short-Term Memory (LSTM) and modified Transformer deep learning models, and*
 302 *the conceptual Sacramento Soil Moisture Accounting (SAC-SMA), with units in mm/day and one*
 303 *specific seed (rather than a random seed). The figure depicts the following comparisons: (a) Nash-Sutcliffe Efficiency (NSE) vs*
 304 *CDF, (b) Kling-Gupta Efficiency (KGE) vs CDF, (c) Low flow percent bias (FLV) vs CDF, and (d)*
 305 *High flow percent bias (FHV) vs CDF. Single-forcing models were implemented on a set of 671*
 306 *basins in the CAMELS dataset, whereas multi-forcing models were applied to a subset of 531*
 307 *basins from that dataset.*

309
310
311
312
313
314
315
316
317
318
319

Table 1. Comparative performance metrics for single and multi-forcing experiments with LSTM, vanilla Transformer, and modified Transformer models. We conducted an evaluation of single forcing on 671 basins and multi-forcing on 531 basins, employing the LSTM model results from Kratzert et al., 2019, originally evaluated on 531 basins. To broaden our insights into the impacts of single-forcing on the entire CAMELS dataset and make a fair comparison, we retrained their model on an expanded set of 671 basins with single NLDAS dataset. These numbers are only very slightly different from Kratzert et al., 2019. The means for Kling-Gupta Efficiency (KGE), high flow percent bias (FHV), and low flow percent bias (FLV) are averages from the 10 different ensemble members, each with a different random seed, while the standard deviations (std) for KGE, FHV and FLV are calculated for the ensemble members.

	Forcing: NLDAS			Forcing: Multi-forcing		
	LSTM	Vanilla Transformer	Modified Transformer	LSTM	Vanilla Transformer	Modified Transformer
KGE (mean \pm std)	0.73 \pm 0.003	0.71 \pm 0.007	0.74 \pm 0.007	0.80 \pm 0.004	0.77 \pm 0.016	0.80 \pm 0.007
FHV (mean \pm std)	-17.49 \pm 0.58	-26.66 \pm 2.83	-18.00 \pm 2.94	-11.91 \pm 0.549	-21.54 \pm 2.64	-9.19 \pm 4.01
FLV (mean \pm std)	-2.82 \pm 8.15	3.31 \pm 2.34	2.28 \pm 4.24	2.57 \pm 4.072	0.77 \pm 1.65	2.72 \pm 2.41

320
321
322

323 The SCA-SMA model had the lowest performance across all experiments, and aligns consistently
324 with the results of Feng et al. (2020) and Kratzert et al. (2021). For the single-forcing CAMELS
325 benchmark (671 basins), the vanilla Transformer was outperformed by LSTM (Table 1; Figure 2).
326 Overall, the vanilla Transformer fell behind LSTM in all metrics, although not by much. Looking at
327 Kling-Gupta Efficiency, the vanilla Transformer achieved a value of 0.71, compared to 0.73 for
328 the LSTM. These results suggest that, without modification, the vanilla Transformer is missing
329 some critical ability to simulate hydrologic processes.

330

331 The vanilla Transformer's under-performance is a curious case as it has been widely recognized
332 that "attention is all you need" (Vaswani et al., 2017) in sequential modeling, and we have several

333 interpretations of the results presented here. First, it is possible that the dataset size is too small
334 here and advantages for the Transformer could emerge for larger quantities of data. Second, the
335 natural hydrologic process is a “Markovian” system (Grey Nearing, personal communication)
336 where the states at the current time step, rather than more remotely-in-the-past steps, completely
337 determine the system’s trajectory for future time steps (along with the forcings). To be more
338 concrete, the soil moisture today, rather than that from any previous days, would have far more
339 of an impact on tomorrow’s streamflow discharge. This is in strong contrast to human languages
340 where the order of the words can often be inverted without changing the context, which would
341 favor the attention-based Transformer architecture. Third, the accumulation of water and its
342 nonlinear interactions makes memory effects important, but the Transformer does not have
343 memory and is not necessarily strong at capturing the effects of memory. Regardless of the
344 reason, the results mean that the vanilla Transformer is not optimal for streamflow predictions at
345 the very least, and further changes are likely needed in order to use it for modeling natural
346 systems.

347

348 On the other hand, the modified Transformer demonstrates performance metrics that are
349 comparable to or slightly surpass those of the LSTM. However, it exhibits greater variability
350 among ensemble members, indicated by the standard deviation of the KGE metric: ± 0.003 for the
351 LSTM and ± 0.007 for the modified Transformer. Its KGE (0.74) is slightly higher than LSTM (0.73),
352 and the differences in FLV and FHV from LSTM’s values are too small to call an advantage
353 considering their variability. As to be discussed below, while these differences are small, we
354 simply should not expect larger differences as the possible room of improvement may be very
355 small at this stage. The ensemble standard deviation of KGE is 0.003 with LSTM and 0.007 with
356 the modified Transformer. The LSTM has a smaller ensemble standard deviation for FHV than
357 the modified Transformer, while the opposite is true for FLV. The ensemble standard deviation of
358 median FHV is 0.58 for LSTM and 2.94 for the modified Transformer, while this value for the FLV

359 is 8.15 for the LSTM and 4.24 for the modified Transformer. This suggests that while we obtain
360 very similar overall metrics, the LSTM and the modified Transformer preferentially address
361 different parts of the hydrograph in this experiment. LSTM more reliably focuses on the high-flow
362 regime (quantified by the smaller ensemble standard deviation of FHV) than the modified
363 Transformer, but the latter can better capture the long-term dependence (quantified by ensemble
364 standard deviation of FLV representing groundwater baseflow). It seems there is some tradeoff
365 for the different flow regimes.

366

367 The multi-forcing experiment generally shows similar patterns: the vanilla Transformer falls behind
368 the other two models, which have very similar ensemble-mean performance metrics but different
369 ensemble standard deviations. The high KGE (0.80) and slightly better-than-LSTM FHV (9.19) for
370 the modified Transformer demonstrates that it, too, is able to fuse different forcing datasets as
371 can LSTM, which no other model architecture has shown. Just as in the single-forcing NLDAS
372 experiment, the modified Transformer has a larger stochastic variability (quantified by ensemble
373 standard deviation) for FHV but smaller variability for FLV. Because both FHV and FLV have
374 improved compared to the single-forcing experiment, the modified Transformer was able to utilize
375 the short-term and long-term dependencies of multiple forcing datasets. For one particular
376 ensemble member (based on different random seeds), the cumulative density plot shows very
377 similar curves between the modified Transformer and LSTM models.

378

379 The high agreement between the two model architectures, both of which are state of the art,
380 suggests that we are likely at or very close to the predictive limit of the CAMELS dataset for this
381 test (temporal test, training in one time period and testing in another). We suspect that unless we
382 bring in new information, it is highly unlikely for any other models to produce noticeable
383 advantages beyond these two models on this dataset, for the tests presented here. Errors with
384 forcing, basin shapes, attribute, and discharge data are likely the remaining factors preventing

385 higher performance. It should be mentioned that for another test, e.g., prediction in ungauged
386 regions or spatial extrapolation, physics-informed hybrid models (called differentiable models
387 (Shen et al., 2023)) can actually outperform LSTM (Aboelyazeed et al., 2023; Feng et al., 2022;
388 Feng, Beck, Lawson, et al., 2023; Tsai et al., 2021). Moreover, several issues surrounding the
389 CAMELS dataset include using basin-average attributes that cannot resolve subbasin-level
390 spatial heterogeneity, using daily precipitation that does not represent hourly rainfall intensity, a
391 fraction of basins having major reservoirs, and the inclusion of some overly large basins.

392

393 Nevertheless, exactly because the Transformer algorithm does not have time integration, it can
394 be trained in a highly parallel fashion and is suited to learning from large amounts of data. As the
395 amount of data and the amount of neurons increase, it is possible to observe emergent behaviors
396 of intelligence (Bubeck et al., 2023). This is a property that is worth further exploring in future
397 studies in hydrology and geosciences. We leave to future work the question of how to incorporate
398 more data with the modified Transformer, and testing this architecture on spatial extrapolation (for
399 data-scarce scenarios) (Feng et al., 2021) and temporal extrapolation (for multidecadal projection
400 of trends).

401

402 While some studies claim that Transformer models surpass LSTM models in performance, their
403 evaluations are often limited to small datasets (Abed et al., 2022; Amanambu et al., 2022;
404 Ghobadi & Kang, 2022), forecasting experiments (Yin et al., 2022), or still incorporate a mix of
405 recurrent neural networks and attention mechanisms (Koya & Roy, 2023) (hereafter called KR23).
406 KR23 evaluated the global Caravan dataset using the TFT model, yet several aspects of their
407 approach hinder direct comparison. Firstly, FR23's comparison on a global dataset is valuable
408 and welcomed, as they reported median KGE of 0.705 on 2610 basins for LSTM (basin-by-basin
409 training) across the entire Caravan dataset, but did not provide results for the CAMELS dataset.
410 When LSTM was benchmarked on a similar global dataset in another paper (Feng, Beck, de

411 Bruijn, et al., 2023) but was trained and tested for all basins simultaneously, it obtained a median
412 KGE of 0.78 for 1675 basins with long-term records, far higher than the KGE of 0.647 reported in
413 KR23, presumably due to using the practice of training on all basins simultaneously (Fang et al.,
414 2022; Kratzert et al., 2024). Secondly, with the addition of LSTM units in KR23’s TFT, it is unclear
415 how much the attention mechanisms helped performance in contrast to the LSTM units. Moreover,
416 their model, being a hybrid of RNN and attention, still faces challenges with parallelization issues.
417 Finally, they employed cubic spline interpolation on the streamflow data, which smooths the target
418 data and undermines the comparability of model results. To validate our perspective, we
419 employed the TFT model from PyTorch Forecasting (Beitner, 2020) on the CAMELS dataset and
420 observed that the model’s training speed was significantly slower, with each epoch taking 30 times
421 longer than LSTM. We welcome the community to benchmark on shared datasets with
422 transparent basin list and input list.

423

424 ***Conclusions***

425 In this work, we compared a vanilla Transformer encoder and a modified Transformer to the
426 current state-of-the-art model, LSTM, on the CAMELS benchmark dataset. The vanilla
427 Transformer seems to miss some critical functionality so that it is not optimal for simulating
428 streamflow. The modified Transformer with no recurrent connection obtains slightly more
429 favorable results (albeit only with a scale advantage) than LSTM. These results already represent
430 rare competitive results to the LSTM in rigorous community-shared benchmarks. This means we
431 can technically continue to search for better architecture to further improve its performance and
432 suitability for natural physical systems, as the current setup may not yet be optimal. Nevertheless,
433 the differences are overall small between the models, and we may already be very close to the
434 optimum for this dataset with this test. On the one hand, we do not expect any architectural
435 change to result in any significant improvement (to be more precise, on the order of 0.02 for KGE).

436 An expansion of the dataset, e.g., better descriptors or forcing dataset will be required to obtain
437 substantial prediction improvements. On the other hand, the modified Transformer architecture is
438 a viable alternative to LSTM and may find advantages for larger datasets in the future. The
439 transformer architecture's advantages may not reside with sequential information extraction but
440 with serving as a foundational model to capture the joint distribution, accumulate knowledge and
441 extract deep, abstract and complex concepts. These advantages should be explored in future
442 hydrologic and geoscientific research.

443

444 ***Funding***

445 JL is supported by National Science Foundation EAR-2221880 and the U.S. Department of
446 Energy under award DE-SC0016605. KL and CS are supported by Cooperative Institute for
447 Research to Operations in Hydrology (CIROH) through the NOAA Cooperative Agreement with
448 The University of Alabama (NA22NWS4320003) and subaward A22-0307-S003.

449 ***Data availability and sharing***

450 All data used for the analysis in this work is publicly available and is cited respectively. An
451 updated zenodo code release will be uploaded upon manuscript acceptance.

452

453 ***Competing Interests***

454 CS and KL have financial interests in HydroSapient, Inc., a company which could potentially
455 benefit from the results of this research. This interest has been reviewed by the University in
456 accordance with its Individual Conflict of Interest policy, for the purpose of maintaining the
457 objectivity and the integrity of research at The Pennsylvania State University.

458

459

460 **Bibliography**

461 Abed, M., Imteaz, M. A., Ahmed, A. N., & Huang, Y. F. (2022). A novel application of
462 transformer neural network (TNN) for estimating pan evaporation rate. *Applied Water
463 Science*, 13(2), 31. <https://doi.org/10.1007/s13201-022-01834-w>

464 Aboelyazeed, D., Xu, C., Hoffman, F. M., Liu, J., Jones, A. W., Rackauckas, C., et al. (2023). A
465 differentiable, physics-informed ecosystem modeling and learning framework for large-
466 scale inverse problems: demonstration with photosynthesis simulations. *Biogeosciences*,
467 20(13), 2671–2692. <https://doi.org/10.5194/bg-20-2671-2023>

468 Addor, N., Newman, A. J., Mizukami, N., & Clark, M. P. (2017). Catchment Attributes and
469 MEteorology for Large-Sample studies (CAMELS) version 2.0 [Data set]. Dataset,
470 Boulder, CO: UCAR/NCAR. <https://doi.org/10.5065/D6G73C3Q>

471 Afzaal, H., Farooque, A. A., Abbas, F., Acharya, B., & Esau, T. (2020). Groundwater estimation
472 from major physical hydrology components using artificial neural networks and deep
473 learning. *Water*, 12(1), 5. <https://doi.org/10.3390/w12010005>

474 Amanambu, A. C., Mossa, J., & Chen, Y.-H. (2022). Hydrological Drought Forecasting Using a
475 Deep Transformer Model. *Water*, 14(22), 3611. <https://doi.org/10.3390/w14223611>

476 Anderson, M. G., & McDonnell, J. J. (2005). Sacramento Soil Moisture Accounting Model (SAC-
477 SMA). In *Encyclopedia of Hydrological Sciences*. Chichester, UK: John Wiley & Sons,
478 Ltd. <https://doi.org/10.1002/0470848944.hsa279>

479 Beitner, J. (2020, October 12). PyTorch Forecasting. Retrieved from
480 <https://github.com/jdb78/pytorch-forecasting>

481 Botterill, T. E., & McMillan, H. K. (2023). Using machine learning to identify hydrologic
482 signatures with an encoder–decoder framework. *Water Resources Research*, 59(3),
483 e2022WR033091. <https://doi.org/10.1029/2022WR033091>

484 Bubeck, S., Chandrasekaran, V., Eldan, R., Gehrke, J., Horvitz, E., Kamar, E., et al. (2023,
485 March 27). Sparks of Artificial General Intelligence: Early experiments with GPT-4. arXiv.
486 <https://doi.org/10.48550/arXiv.2303.12712>

487 Burnash, R. J. C., Fernal, R. L., & McGuire, R. A. (1973). *A generalized streamflow simulation*
488 *system: conceptual modeling for digital computers*. Sacramento, Calif.: U. S. Dept. of
489 Commerce, National Weather Service.

490 Carion, N., Massa, F., Synnaeve, G., Usunier, N., Kirillov, A., & Zagoruyko, S. (2020, May 28).
491 End-to-End Object Detection with Transformers. arXiv.
492 <https://doi.org/10.48550/arXiv.2005.12872>

493 Castangia, M., Grajales, L. M. M., Aliberti, A., Rossi, C., Macii, A., Macii, E., & Patti, E. (2023).
494 Transformer neural networks for interpretable flood forecasting. *Environmental Modelling*
495 & Software, 160, 105581. <https://doi.org/10.1016/j.envsoft.2022.105581>

496 Dai, S., Li, L., & Li, Z. (2019). Modeling vehicle interactions via modified LSTM models for
497 trajectory prediction. *IEEE Access*, 7, 38287–38296.
498 <https://doi.org/10.1109/ACCESS.2019.2907000>

499 Dehghani, M., Gouws, S., Vinyals, O., Uszkoreit, J., & Kaiser, Ł. (2019, March 5). Universal
500 Transformers. arXiv. <https://doi.org/10.48550/arXiv.1807.03819>

501 Devlin, J., Chang, M.-W., Lee, K., & Toutanova, K. (2019, May 24). BERT: Pre-training of Deep
502 Bidirectional Transformers for Language Understanding. arXiv.
503 <https://doi.org/10.48550/arXiv.1810.04805>

504 Fang, K., Shen, C., Kifer, D., & Yang, X. (2017). Prolongation of SMAP to spatiotemporally
505 seamless coverage of continental U.S. using a deep learning neural network.
506 *Geophysical Research Letters*, 44(21), 11,030-11,039.
507 <https://doi.org/10.1002/2017gl075619>

508 Fang, K., Kifer, D., Lawson, K., Feng, D., & Shen, C. (2022). The data synergy effects of time-
509 series deep learning models in hydrology. *Water Resources Research*, 58(4),
510 e2021WR029583. <https://doi.org/10.1029/2021WR029583>

511 Feng, D., Fang, K., & Shen, C. (2020). Enhancing streamflow forecast and extracting insights
512 using long-short term memory networks with data integration at continental scales.
513 *Water Resources Research*, 56(9), e2019WR026793.
514 <https://doi.org/10.1029/2019WR026793>

515 Feng, D., Lawson, K., & Shen, C. (2021). Mitigating prediction error of deep learning streamflow
516 models in large data-sparse regions with ensemble modeling and soft data. *Geophysical*
517 *Research Letters*, 48(14), e2021GL092999. <https://doi.org/10.1029/2021GL092999>

518 Feng, D., Liu, J., Lawson, K., & Shen, C. (2022). Differentiable, learnable, regionalized process-
519 based models with multiphysical outputs can approach state-of-the-art hydrologic
520 prediction accuracy. *Water Resources Research*, 58(10), e2022WR032404.
521 <https://doi.org/10.1029/2022WR032404>

522 Feng, D., Beck, H., Lawson, K., & Shen, C. (2023). The suitability of differentiable, physics-
523 informed machine learning hydrologic models for ungauged regions and climate change
524 impact assessment. *Hydrology and Earth System Sciences*, 27(12), 2357–2373.
525 <https://doi.org/10.5194/hess-27-2357-2023>

526 Feng, D., Beck, H., de Bruijn, J., Sahu, R. K., Satoh, Y., Wada, Y., et al. (2023, October 5).
527 Deep dive into global hydrologic simulations: Harnessing the power of deep learning and
528 physics-informed differentiable models (δ HBV-globe1.0-hydroDL). *Geoscientific Model*
529 *Development Discussions*. <https://doi.org/10.5194/gmd-2023-190>

530 Ghobadi, F., & Kang, D. (2022). Improving long-term streamflow prediction in a poorly gauged
531 basin using geo-spatiotemporal mesoscale data and attention-based deep learning: A
532 comparative study. *Journal of Hydrology*, 615, 128608.
533 <https://doi.org/10.1016/j.jhydrol.2022.128608>

534 Gupta, H. V., Kling, H., Yilmaz, K. K., & Martinez, G. F. (2009). Decomposition of the mean
535 squared error and NSE performance criteria: Implications for improving hydrological
536 modelling. *Journal of Hydrology*, 377(1), 80–91.
537 <https://doi.org/10.1016/j.jhydrol.2009.08.003>

538 Hochreiter, S. (1991). *Untersuchungen zu dynamischen neuronalen Netzen*. Institut fur
539 Informatik, Technische Universitat, Munchen, 1-150. Retrieved from
540 <https://www.semanticscholar.org/paper/Untersuchungen-zu-dynamischen-neuronalen-Netzen-Hochreiter/3f3d13e95c25a8f6a753e38dfce88885097cbd43>

542 Hochreiter, S., & Schmidhuber, J. (1997). Long Short-Term Memory. *Neural Computation*, 9(8),
543 1735–1780. <https://doi.org/10.1162/neco.1997.9.8.1735>

544 Hochreiter, S., Bengio, Y., Frasconi, P., & Jürgen Schmidhuber. (2001). Gradient Flow in
545 Recurrent Nets: The Difficulty of Learning Long-Term Dependencies. In S. C. Kremer &
546 J. F. Kolen (Eds.), *A Field Guide to Dynamical Recurrent Neural Networks* (pp. 237–
547 244). Piscataway, NJ, USA: IEEE Press.

548 Hrachowitz, M., & Clark, M. P. (2017). HESS Opinions: The complementary merits of competing
549 modelling philosophies in hydrology. *Hydrology and Earth System Sciences*, 21(8),
550 3953–3973. <https://doi.org/10.5194/hess-21-3953-2017>

551 Huang, C.-Z. A., Vaswani, A., Uszkoreit, J., Shazeer, N., Simon, I., Hawthorne, C., et al. (2018,
552 December 12). Music Transformer. arXiv. <https://doi.org/10.48550/arXiv.1809.04281>

553 Karita, S., Chen, N., Hayashi, T., Hori, T., Inaguma, H., Jiang, Z., et al. (2019). A Comparative
554 Study on Transformer vs RNN in Speech Applications. In *2019 IEEE Automatic Speech
555 Recognition and Understanding Workshop (ASRU)* (pp. 449–456).
556 <https://doi.org/10.1109/ASRU46091.2019.9003750>

557 Konapala, G., Kao, S.-C., Painter, S. L., & Lu, D. (2020). Machine learning assisted hybrid
558 models can improve streamflow simulation in diverse catchments across the

559 conterminous US. *Environmental Research Letters*, 15(10), 104022.

560 <https://doi.org/10.1088/1748-9326/aba927>

561 Koya, S. R., & Roy, T. (2023, May 20). Temporal Fusion Transformers for Streamflow

562 Prediction: Value of Combining Attention with Recurrence. arXiv.

563 <https://doi.org/10.48550/arXiv.2305.12335>

564 Kratzert, F., Klotz, D., Shalev, G., Klambauer, G., Hochreiter, S., & Nearing, G. (2019). Towards

565 learning universal, regional, and local hydrological behaviors via machine learning

566 applied to large-sample datasets. *Hydrology and Earth System Sciences*, 23(12), 5089–

567 5110. <https://doi.org/10.5194/hess-23-5089-2019>

568 Kratzert, F., Klotz, D., Hochreiter, S., & Nearing, G. S. (2021). A note on leveraging synergy in

569 multiple meteorological data sets with deep learning for rainfall–runoff modeling.

570 *Hydrology and Earth System Sciences*, 25(5), 2685–2703. <https://doi.org/10.5194/hess-25-2685-2021>

572 Kratzert, F., Nearing, G., Addor, N., Erickson, T., Gauch, M., Gilon, O., et al. (2023). Caravan -

573 A global community dataset for large-sample hydrology. *Scientific Data*, 10(1), 61.

574 <https://doi.org/10.1038/s41597-023-01975-w>

575 Kratzert, F., Gauch, M., Klotz, D., & Nearing, G. (2024). HESS Opinions: Never train an LSTM

576 on a single basin. *Hydrology and Earth System Sciences Discussions*, 1–19.

577 <https://doi.org/10.5194/hess-2023-275>

578 Li, Y., & Yang, J. (2019). Hydrological time series prediction model based on attention-LSTM

579 neural network. In *Proceedings of the 2019 2nd International Conference on Machine*

580 *Learning and Machine Intelligence* (pp. 21–25). New York, NY, USA: Association for

581 Computing Machinery. <https://doi.org/10.1145/3366750.3366756>

582 Liu, C., Liu, D., & Mu, L. (2022). Improved Transformer Model for Enhanced Monthly Streamflow

583 Predictions of the Yangtze River. *IEEE Access*, 10, 58240–58253.

584 <https://doi.org/10.1109/ACCESS.2022.3178521>

585 Liu, J., Rahmani, F., Lawson, K., & Shen, C. (2022). A multiscale deep learning model for soil
586 moisture integrating satellite and in situ data. *Geophysical Research Letters*, 49(7),
587 e2021GL096847. <https://doi.org/10.1029/2021GL096847>

588 Liu, J., Hughes, D., Rahmani, F., Lawson, K., & Shen, C. (2023). Evaluating a global soil
589 moisture dataset from a multitask model (GSM3 v1.0) with potential applications for crop
590 threats. *Geoscientific Model Development*, 16(5), 1553–1567.
591 <https://doi.org/10.5194/gmd-16-1553-2023>

592 Maurer, E. P., Wood, A. W., Adam, J. C., Lettenmaier, D. P., & Nijssen, B. (2002). A long-term
593 hydrologically based dataset of land surface fluxes and states for the conterminous
594 United States. *Journal of Climate*, 15(22), 3237–3251. [https://doi.org/10.1175/1520-0442\(2002\)015<3237:ALTHBD>2.0.CO;2](https://doi.org/10.1175/1520-0442(2002)015<3237:ALTHBD>2.0.CO;2)

596 Nash, J. E., & Sutcliffe, J. V. (1970). River flow forecasting through conceptual models part I —
597 A discussion of principles. *Journal of Hydrology*, 10(3), 282–290.
598 [https://doi.org/10.1016/0022-1694\(70\)90255-6](https://doi.org/10.1016/0022-1694(70)90255-6)

599 Newman, A. J., Sampson, K., Clark, M. P., Bock, A., Viger, R. J., & Blodgett, D. (2014). A large-
600 sample watershed-scale hydrometeorological dataset for the contiguous USA. *Boulder*.
601 <https://doi.org/10.5065/D6MW2F4D>

602 Papacharalampous, G., Tyralis, H., & Koutsoyiannis, D. (2018). One-step ahead forecasting of
603 geophysical processes within a purely statistical framework. *Geoscience Letters*, 5(1),
604 12. <https://doi.org/10.1186/s40562-018-0111-1>

605 Pasquiou, A., Lakretz, Y., Hale, J., Thirion, B., & Pallier, C. (2022, July 7). Neural Language
606 Models are not Born Equal to Fit Brain Data, but Training Helps. arXiv.
607 <https://doi.org/10.48550/arXiv.2207.03380>

608 Raganato, A., & Tiedemann, J. (2018). An analysis of encoder representations in transformer-
609 based machine translation. In *Proceedings of the 2018 EMNLP Workshop BlackboxNLP*:

610 *Analyzing and Interpreting Neural Networks for NLP* (pp. 287–297). Brussels, Belgium:
611 Association for Computational Linguistics. <https://doi.org/10.18653/v1/W18-5431>

612 Rahmani, F., Shen, C., Oliver, S., Lawson, K., & Appling, A. (2021). Deep learning approaches
613 for improving prediction of daily stream temperature in data-scarce, unmonitored, and
614 dammed basins. *Hydrological Processes*, 35(11), e14400.
615 <https://doi.org/10.1002/hyp.14400>

616 Rahmani, F., Lawson, K., Ouyang, W., Appling, A., Oliver, S., & Shen, C. (2021). Exploring the
617 exceptional performance of a deep learning stream temperature model and the value of
618 streamflow data. *Environmental Research Letters*, 16(2), 024025.
619 <https://doi.org/10.1088/1748-9326/abd501>

620 Rajpurkar, P., Jia, R., & Liang, P. (2018). Know What You Don't Know: Unanswerable
621 Questions for SQuAD. In *Proceedings of the 56th Annual Meeting of the Association for*
622 *Computational Linguistics (Volume 2: Short Papers)* (pp. 784–789). Melbourne,
623 Australia: Association for Computational Linguistics. <https://doi.org/10.18653/v1/P18-2124>

625 Rives, A., Meier, J., Sercu, T., Goyal, S., Lin, Z., Liu, J., et al. (2021). Biological structure and
626 function emerge from scaling unsupervised learning to 250 million protein sequences.
627 *Proceedings of the National Academy of Sciences*, 118(15), e2016239118.
628 <https://doi.org/10.1073/pnas.2016239118>

629 Shen, C., Appling, A. P., Gentine, P., Bandai, T., Gupta, H., Tartakovsky, A., et al. (2023).
630 Differentiable modelling to unify machine learning and physical models for geosciences.
631 *Nature Reviews Earth & Environment*, 4(8), 552–567. <https://doi.org/10.1038/s43017-023-00450-9>

633 Sun, A. Y., Jiang, P., Mudunuru, M. K., & Chen, X. (2021). Explore spatio-temporal learning of
634 large sample hydrology using graph neural networks. *Water Resources Research*,
635 57(12), e2021WR030394. <https://doi.org/10.1029/2021WR030394>

636 Thornton, P. E., Running, S. W., & White, M. A. (1997). Generating surfaces of daily
637 meteorological variables over large regions of complex terrain. *Journal of Hydrology*,
638 190(3), 214–251. [https://doi.org/10.1016/S0022-1694\(96\)03128-9](https://doi.org/10.1016/S0022-1694(96)03128-9)

639 Tsai, W.-P., Feng, D., Pan, M., Beck, H., Lawson, K., Yang, Y., et al. (2021). From calibration to
640 parameter learning: Harnessing the scaling effects of big data in geoscientific modeling.
641 *Nature Communications*, 12(1), 5988. <https://doi.org/10.1038/s41467-021-26107-z>

642 Vaswani, A., Shazeer, N., Parmar, N., Uszkoreit, J., Jones, L., Gomez, A. N., et al. (2017,
643 December 5). Attention Is All You Need. arXiv.
644 <https://doi.org/10.48550/arXiv.1706.03762>

645 Wunsch, A., Liesch, T., & Broda, S. (2022). Deep learning shows declining groundwater levels
646 in Germany until 2100 due to climate change. *Nature Communications*, 13(1), 1221.
647 <https://doi.org/10.1038/s41467-022-28770-2>

648 Xia, Y., Mitchell, K., Ek, M., Sheffield, J., Cosgrove, B., Wood, E., et al. (2012). Continental-
649 scale water and energy flux analysis and validation for the North American Land Data
650 Assimilation System project phase 2 (NLDAS-2): 1. Intercomparison and application of
651 model products. *Journal of Geophysical Research: Atmospheres*, 117(D3).
652 <https://doi.org/10.1029/2011JD016048>

653 Xiang, Z., & Demir, I. (2020). Distributed long-term hourly streamflow predictions using deep
654 learning – A case study for State of Iowa. *Environmental Modelling & Software*, 131,
655 104761. <https://doi.org/10.1016/j.envsoft.2020.104761>

656 Xu, Z., Wang, S., Stanislawski, L. V., Jiang, Z., Jaroenchai, N., Sainju, A. M., et al. (2021). An
657 attention U-Net model for detection of fine-scale hydrologic streamlines. *Environmental
658 Modelling & Software*, 140, 104992. <https://doi.org/10.1016/j.envsoft.2021.104992>

659 Yang, E., Li, M. D., Raghavan, S., Deng, F., Lang, M., Succi, M. D., et al. (2023). Transformer
660 versus traditional natural language processing: how much data is enough for automated

radiology report classification? *The British Journal of Radiology*, 20220769.
<https://doi.org/10.1259/bjr.20220769>

Yang, H., Zhang, Z., Liu, X., & Jing, P. (2023). Monthly-scale hydro-climatic forecasting and climate change impact evaluation based on a novel DCNN-Transformer network. *Environmental Research*, 236, 116821. <https://doi.org/10.1016/j.envres.2023.116821>

Yilmaz, K. K., Gupta, H. V., & Wagener, T. (2008). A process-based diagnostic approach to model evaluation: Application to the NWS distributed hydrologic model. *Water Resources Research*, 44(9). <https://doi.org/10/fpvsgb>

Yin, H., Guo, Z., Zhang, X., Chen, J., & Zhang, Y. (2022). RR-Former: Rainfall-runoff modeling based on Transformer. *Journal of Hydrology*, 609, 127781.
<https://doi.org/10.1016/j.jhydrol.2022.127781>

Yin, H., Zhu, W., Zhang, X., Xing, Y., Xia, R., Liu, J., & Zhang, Y. (2023). Runoff predictions in new-gauged basins using two transformer-based models. *Journal of Hydrology*, 622, 129684. <https://doi.org/10.1016/j.jhydrol.2023.129684>

Zhang, Y., Chen, G., Yu, D., Yao, K., Khudanpur, S., & Glass, J. (2016). Highway long short-term memory RNNs for distant speech recognition. In *2016 IEEE international conference on acoustics, speech and signal processing (ICASSP)* (pp. 5755–5759). IEEE. <https://doi.org/10.1109/ICASSP.2016.7472780>

Zhou, H., Zhang, S., Peng, J., Zhang, S., Li, J., Xiong, H., & Zhang, W. (2021). Informer: Beyond efficient transformer for long sequence time-series forecasting. In *Proceedings of the AAAI conference on artificial intelligence* (Vol. 35, pp. 11106–11115). Retrieved from <https://ojs.aaai.org/index.php/AAAI/article/view/17325>